UNSTEADY MHD FREE CONVECTION FLOW PAST AN INFINITE VERTICAL PLATE WITH VISCOUS DISSIPATION AND HEAT ABSORPTION

K. Anitha[1*], S. Venkataramana[1] and S. Sivaiah[2]

[1]Department of Mathematics, Sri Venkateswara University, Tirupati-517 502, A.P., India
[2]Department of Engineering Mathematics, GITAM University, Hyderabad Campus, Hyderabad – 502 329, A.P., India

ABSTRACT

In this paper, we study the effects of viscous dissipation and heat absorption on unsteady MHD free convection flow of a viscous, incompressible, electrically-conducting fluid past an infinite vertical porous plate. The dimensionless governing equations are solved by Finite element technique. Numerical evaluation of the analytical results is performed. Graphical results for velocity, temperature and concentration profiles and tabulated results for skin friction coefficient, Nusselt number and Sherwood number are presented and discussed.

Key Words: Unsteady, MHD, Heat absorption, Viscous dissipation, Finite element method.

1. INTRODUCTION

In recent years, the analysis of hydromagnetic convection flow involving heat and mass transfer in porous medium has attracted the attention of many scholars because of its possible applications in diverse fields of science and technology such as–soil sciences, astrophysics, geophysics, nuclear power reactors etc. In geophysics, it finds its applications in the design of MHD generators and accelerators, underground water energy storage system etc. It is worth-mentioning that MHD is now undergoing a stage of great enlargement and differentiation of subject matter. These new problems draw the attention of the researchers due to their varied significance, in liquid metals, electrolytes and ionized gases etc. The MHD in the present form is due to contributions of several notable authors like Shercliff [18], Ferraro and Plumpton [9] and Crammer and Pai [8]. Prasad *et al.* [14] discussed finite difference analysis of radiative free convection flow past an impulsively started vertical plate with variable heat and mass flux. Suneetha *et al.* [22] discussed radiation and mass transfer effects on MHD free convective Dissipative fluid in the presence of heat source/sink. Prasad *et al.* [15] studied transient radiative hydromagnetic free convection flow past an impulsively started vertical plate with uniform heat and mass flux. Singh *et al.* [19] studied the effects of permeability variation and oscillatory suction velocity on free convection and mass transfer flow of a viscous fluid past an infinite vertical porous plate to a porous medium when the plate is subjected to a time dependent suction velocity normal to the plate in the presence of uniform transverse magnetic field. Ahmed and Liu [1] studied the effect of heat and mass transfer mixed convective three-dimensional flow with transversely periodic suction velocity. The effect of chemical reaction magnetohydrodynamic flow of a uniformly stretched vertical permeable surface in the presence of heat generation/absorption studied by Chamkha [6]. Ahmed [2] presented the effects of viscous dissipation and chemical reaction on transient free convective MHD flow over a vertical porous plate. Chen [7] discussed the combined heat and mass transfer in MHD free convection from a vertical plate with ohmic heating and viscous dissipation.

The propagation of thermal energy through mercury and electrolytic solution in the presence of external magnetic field and heat absorbing sinks has wide range of applications in chemical and aeronautical engineering, atomic propulsion, space science etc. Ahmed [3] studied free and forced convective MHD oscillatory flows over an infinite porous surface in an oscillating free stream. Transient three–dimensional flows through a porous medium with transverse permeability oscillating with time studied by Ahmed [4]. Aldoss and Al-Nimir [5] has been studied the effect of the local acceleration term on the MHD transient free convection flow over a vertical plate. Muthucumaraswamy *et al.* [13] studied the heat and mass transfer effects on flow past an impulsively started vertical plate. J.A. Rao and S.Sivaiah [16] discussed the effects of chemical reaction on unsteady MHD flow past semi infinite vertical porous plate with viscous dissipation. Effects of the chemical reaction and radiation absorption on free convective flow through porous medium with variable suction in the presence of uniform magnetic field were studied by sudheer babu and satyanarayana [21].

Corresponding author: K. Anitha[1*]
[1]Department of Mathematics, Sri Venkateswara University, Tirupati-517 502, A.P., India

In most of the studies mentioned above, viscous dissipation is neglected. Gebhart [11] has shown the importance of viscous dissipative heat in free convection flow in the case of isothermal and constant heat flux at the plates. Gebhart and Mollendorf [10] considered the effects of viscous dissipation for external natural convection flow over a surface. Soundalgekar [20] analyzed viscous dissipative heat on the two dimensional unsteady free convective flow past an infinite vertical porous plate when the temperature oscillates in time and there is constant suction at the plate. Israel Cookey et al. [12] investigated the influence of viscous dissipation and radiation on unsteady MHD free convection flow past an infinite heated vertical plate in a porous medium with time dependent suction.

The objective of the present paper is to analyze the effects of viscous dissipation and heat absorption on unsteady MHD free convection flow of a viscous, incompressible, electrically conducting fluid past an infinite vertical porous plate. The equations of continuity, linear momentum, energy and diffusion, which govern the flow field, are solved by Galerkin finite element method. The behavior of the velocity, temperature, concentration, skin-friction, Nusselt number and Sherwood number has been discussed for variations in the governing parameters.

2. FORMULATION OF THE PROBLEM

An unsteady MHD free convective flow of an incompressible, electrically conducting fluid past an infinite vertical porous plate in the presence of viscous dissipation is considered. The x' – axis be taken in the vertically upward direction along the infinite vertical plate and y' – axis normal to it. A uniform magnetic field is applied in the direction perpendicular to the plate. The transverse applied magnetic field and magnetic Reynolds number are assumed to be very small in comparison with the other chemical species which are present, and hence the Soret and Dufour effects are negligible. Neglecting the induced magnetic field and applying Boussinesq's approximation.
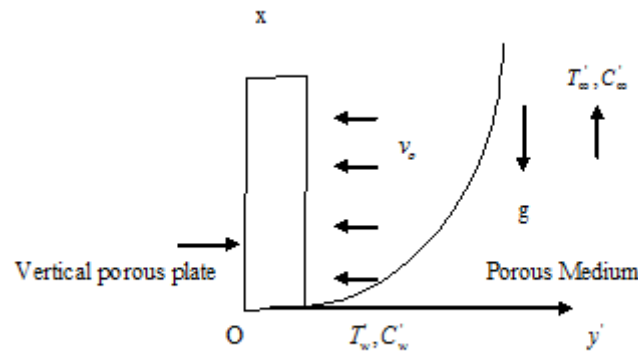

Figure 1. Physical sketch and geometry of the problem

Continuity Equation:

$$\frac{\partial v'}{\partial y'} = 0 \Rightarrow v' = -v'_o \text{ (Constant)} \tag{1}$$

Momentum Equation:

$$\frac{\partial u'}{\partial t'} + v' \frac{\partial u'}{\partial y'} = g\beta\left(T' - T'_\infty\right) - \upsilon \frac{u'}{K'} + g\beta^*\left(C' - C'_\infty\right) + \upsilon \frac{\partial^2 u'}{\partial y'^2} - \frac{\sigma B_o^2}{\rho} u' \tag{2}$$

Energy Equation:

$$\frac{\partial T'}{\partial t'} + v' \frac{\partial T'}{\partial y'} = \frac{k}{\rho C_p} \frac{\partial^2 T'}{\partial y'^2} + \frac{\upsilon}{C_p}\left(\frac{\partial u'}{\partial y'}\right)^2 - \frac{Q'}{\rho C_p}\left(T' - T'_\infty\right) \tag{3}$$

Concentration Equation:

$$\frac{\partial C'}{\partial t'} + v' \frac{\partial C'}{\partial y'} = D \frac{\partial^2 C'}{\partial y'^2} \tag{4}$$

The boundary conditions of the problem are:

$$
\left.
\begin{aligned}
&u' = 0, v' = -v'_0, \\
&T' = T'_w + \varepsilon \left(T'_w - T'_\infty \right) e^{i\,\omega' t'} \\
&C' = C'_w + \varepsilon \left(C'_w - C'_\infty \right) e^{i\,\omega' t'} \\
&at\ y' = 0 \\
&u' \to 0, T' \to T'_\infty, C' \to C'_\infty\ as\ y' \to \infty
\end{aligned}
\right\}
\tag{5}
$$

Introducing the following non-dimensional variables and parameters,

$$
\left.
\begin{aligned}
&y = \frac{y' v'_o}{\upsilon},\ t = \frac{t' v'^2_o}{\upsilon},\ \omega = \frac{\upsilon \omega'}{v'^2_o},\ u = \frac{u'}{v'_o},\ M = \left(\frac{\sigma B_o^2}{\rho} \right) \frac{\upsilon}{v'^2_o},\ K = \frac{K' v'^2_0}{\upsilon^2}, \\
&Sc = \frac{\upsilon}{D},\ T = \frac{T' - T'_\infty}{T'_w - T'_\infty}, C = \frac{C' - C'_\infty}{C'_w - C'_\infty}\ \Pr = \frac{\upsilon \rho\, C_p}{k},\ Gr = \frac{\upsilon g \beta \left(T'_w - T'_\infty \right)}{v'^3_o}, \\
&Gm = \frac{\upsilon g \beta^* \left(C'_w - C'_\infty \right)}{v'^3_0} Q = \frac{Q' \upsilon}{\rho\, C_p v'^2_o},\ Ec = \frac{v'^2_o}{C_p \left(T'_w - T'_\infty \right)};
\end{aligned}
\right\}
\tag{6}
$$

where $g,\ \rho, \upsilon,\ \beta,\ \beta^*, \sigma,\ \omega,\ k, T, v'_0, T'_w, T'_\infty,\ C'_w, C'_\infty, C_p,\ \Pr,\ Sc,\ Gr, Gm, Q, K, Ec$ and M are respectively the acceleration due to gravity, density, coefficient of kinematic viscosity, volumetric coefficient of expansion for heat transfer, volumetric coefficient of expansion for mass transfer, electrical conductivity, angular frequency, thermal diffusivity, temperature, scale of suction velocity, temperature at the plate, temperature at infinity, concentration at the plate, concentration at infinity, specific heat at constant pressure, Prandtl number, Schmidt number, Grashof number for heat transfer, Grash of number for mass transfer, heat source parameter, permeability parameter, Eckert number and Hartmann number.

In view of equations (5) and (6) the equations (1), (2), (3) and (4) reduces to the following dimensionless form.

$$
\frac{\partial u}{\partial t} - \frac{\partial u}{\partial y} = (Gr)T + (Gm)C + \frac{\partial^2 u}{\partial y^2} - \left(M + \frac{1}{K} \right) u
\tag{7}
$$

$$
\frac{\partial T}{\partial t} - \frac{\partial T}{\partial y} = \frac{1}{\Pr} \frac{\partial^2 T}{\partial y^2} - QT + (Ec) \left(\frac{\partial u}{\partial y} \right)^2
\tag{8}
$$

$$
\frac{\partial C}{\partial t} - \frac{\partial C}{\partial y} = \frac{1}{Sc} \frac{\partial^2 C}{\partial y^2}
\tag{9}
$$

The corresponding boundary conditions are:

$$
\left.
\begin{aligned}
&u = 0,\ T = 1 + \varepsilon e^{i\omega t}, C = 1 + \varepsilon e^{i\omega t}\ at\ y = 0 \\
&u \to 0,\ T \to 0, C \to 0\ \ \ as\ y \to \infty
\end{aligned}
\right\}
\tag{10}
$$

3. METHOD OF SOLUTION

By applying Galerkin finite element method for equation (6) over the element (e), ($y_j \le y \le y_k$) is:

$$
\int_{y_j}^{y_k} \left\{ N^{(e)T} \left[\frac{\partial^2 u^{(e)}}{\partial y^2} - \frac{\partial u^{(e)}}{\partial t} + \frac{\partial u^{(e)}}{\partial y} - Au^{(e)} + P \right] \right\} dy = 0
\tag{11}
$$

where $P = (Gr)T_i^{\,j} + GmC_i^{\,j}$, $A = M + \frac{1}{K}$;

Integrating the first term in equation (9) by parts one obtains

$$N^{(e)T} \left\{ \frac{\partial u^{(e)}}{\partial y} \right\}_{y_j}^{y_k} - \int_{y_j}^{y_k} \left\{ \frac{\partial N^{(e)T}}{\partial y} \frac{\partial u^{(e)}}{\partial y} + N^{(e)T} \left(\frac{\partial u^{(e)}}{\partial t} - \frac{\partial u^{(e)}}{\partial y} + Au^{(e)} - P \right) \right\} dy = 0 \tag{12}$$

Neglecting the first term in equation (10), one gets:

$$\int_{y_j}^{y_k} \left\{ \frac{\partial N^{(e)T}}{\partial y} \frac{\partial u^{(e)}}{\partial y} + N^{(e)T} \left(\frac{\partial u^{(e)}}{\partial t} - \frac{\partial u^{(e)}}{\partial y} + Au^{(e)} - P \right) \right\} dy = 0$$

Let $u^{(e)} = N^{(e)} \phi^{(e)}$ be the linear piecewise approximation solution over the element (e)

($y_j \le y \le y_k$), where $N^{(e)} = [N_j \quad N_k]$, $\phi^{(e)} = [u_j \quad u_k]^T$ and $N_j = \dfrac{y_k - y}{y_k - y_j}, N_k = \dfrac{y - y_j}{y_k - y_j}$ are the basis functions. One obtains:

$$\int_{y_j}^{y_k} \left\{ \begin{bmatrix} N_j^{'} N_j^{'} & N_j^{'} N_k^{'} \\ N_j^{'} N_k^{'} & N_k^{'} N_k^{'} \end{bmatrix} \begin{bmatrix} u_j \\ u_k \end{bmatrix} \right\} dy + \int_{y_j}^{y_k} \left\{ \begin{bmatrix} N_j N_j & N_j N_k \\ N_j N_k & N_k N_k \end{bmatrix} \begin{bmatrix} \dot{u}_j \\ \dot{u}_k \end{bmatrix} \right\} dy - \int_{y_j}^{y_k} \left\{ \begin{bmatrix} N_j N_j^{'} & N_j N_k^{'} \\ N_j N_k^{'} & N_k N_k^{'} \end{bmatrix} \begin{bmatrix} u_j \\ u_k \end{bmatrix} \right\} dy$$

$$+ A \int_{y_j}^{y_k} \left\{ \begin{bmatrix} N_j N_j & N_j N_k \\ N_j N_k & N_k N_k \end{bmatrix} \begin{bmatrix} u_j \\ u_k \end{bmatrix} \right\} dy = P \int_{y_j}^{y_k} \begin{bmatrix} N_j \\ N_k \end{bmatrix} dy$$

Simplifying we get

$$\frac{1}{l^{(e)2}} \begin{bmatrix} 1 & -1 \\ -1 & 1 \end{bmatrix} \begin{bmatrix} u_j \\ u_k \end{bmatrix} + \frac{1}{6} \begin{bmatrix} 2 & 1 \\ 1 & 2 \end{bmatrix} \begin{bmatrix} \dot{u}_j \\ \dot{u}_k \end{bmatrix} - \frac{1}{2l^{(e)}} \begin{bmatrix} -1 & 1 \\ -1 & 1 \end{bmatrix} \begin{bmatrix} u_j \\ u_k \end{bmatrix} + \frac{A}{6} \begin{bmatrix} 2 & 1 \\ 1 & 2 \end{bmatrix} \begin{bmatrix} u_j \\ u_k \end{bmatrix} = \frac{P}{2} \begin{bmatrix} 1 \\ 1 \end{bmatrix}$$

Where prime and dot denotes differentiation w.r.t 'y' and time 't' respectively. Assembling the element equations for two consecutive elements $y_{i-1} \le y \le y_i$ and $y_i \le y \le y_{i+1}$ following is obtained:

$$\frac{1}{l^{(e)2}} \begin{bmatrix} 1 & -1 & 0 \\ -1 & 2 & -1 \\ 0 & -1 & 1 \end{bmatrix} \begin{bmatrix} u_{i-1} \\ u_i \\ u_{i+1} \end{bmatrix} + \frac{1}{6} \begin{bmatrix} 2 & 1 & 0 \\ 1 & 4 & 1 \\ 0 & 1 & 2 \end{bmatrix} \begin{bmatrix} \dot{u}_{i-1} \\ \dot{u}_i \\ \dot{u}_{i+1} \end{bmatrix} - \frac{1}{2l^{(e)}} \begin{bmatrix} -1 & 1 & 0 \\ -1 & 0 & 1 \\ 0 & -1 & 1 \end{bmatrix} \begin{bmatrix} u_{i-1} \\ u_i \\ u_{i+1} \end{bmatrix}$$

$$+ \frac{A}{6} \begin{bmatrix} 2 & 1 & 0 \\ 1 & 4 & 1 \\ 0 & 1 & 2 \end{bmatrix} \begin{bmatrix} u_{i-1} \\ u_i \\ u_{i+1} \end{bmatrix} = \frac{P}{2} \begin{bmatrix} 1 \\ 2 \\ 1 \end{bmatrix} \tag{13}$$

Now put row corresponding to the node 'i' to zero, from equation (11) the difference schemes with $l^{(e)} = h$ is:

$$\frac{1}{h^2} [-u_{i-1} + 2u_i - u_{i+1}] + \frac{1}{6} [\dot{u}_{i-1} + 4\dot{u}_i + \dot{u}_{i+1}] - \frac{1}{2h} [-u_{i-1} + u_{i+1}] + \frac{A}{6} [u_{i-1} + 4u_i + u_{i+1}] = P \tag{14}$$

Applying the trapezoidal rule, following system of equations in Crank-Nicholson method are obtained :

$$A_1 u_{i-1}^{n+1} + A_2 u_i^{n+1} + A_3 u_{i+1}^{n+1} = A_4 u_{i-1}^n + A_5 u_i^n + A_6 u_{i+1}^n + P^* \tag{15}$$

Now from equation (7) following equation is obtained:

$$B_1 T_{i-1}^{n+1} + B_2 T_i^{n+1} + B_3 T_{i+1}^{n+1} = B_4 T_{i-1}^{n} + B_5 T_i^{n} + B_6 T_{i+1}^{n} + Q^{**}$$ (16)

$$D_1 C_{i-1}^{n+1} + D_2 C_i^{n+1} + D_3 C_{i+1}^{n+1} = D_4 C_{i-1}^{n} + D_5 C_i^{n} + D_6 C_{i+1}^{n}$$ (17)

where $A_1 = 2 + Ak + 3rh - 6r$, $A_2 = 8 + 4Ak + 12r$, $A_3 = 2 + Ak - 3rh - 6r$,

$A_4 = 2 - Ak - 3rh + 6r$, $A_5 = 8 - 4Ak - 12r$, $A_6 = 2 - Ak + 3rh + 6r$,

$B_1 = 2(\text{Pr}) + 3rh(\text{Pr}) - 6r - Q(\text{Pr})k$, $B_2 = 8(\text{Pr}) - 4Q(\text{Pr})k + 12r$,

$B_3 = 2(\text{Pr}) - 3rh(\text{Pr}) - 6r - Q(\text{Pr})k$, $B_4 = 2(\text{Pr}) - 3rh(\text{Pr}) + 6r + Q(\text{Pr})k$,

$B_5 = 8(\text{Pr}) + 4Q(\text{Pr})k - 12r$, $B_6 = 2(\text{Pr}) + 3rh(\text{Pr}) + 6r + Q(\text{Pr})k$, $D_1 = 2(Sc) + 3rh(Sc) - 6r$,

$D_2 = 8(Sc) + 12r$, $D_3 = 2(Sc) - 3rh(Sc) - 6r$, $D_4 = 2(Sc) - 3rh(Sc) + 6r$, $D_5 = 8(Sc) - 12r$,

$D_6 = 2(Sc) + 3rh(Sc) + 6r$, $P^* = 12Pk = 12k(Gr)T_i^{j} + 12k(Gm)C_i^{j}$,

$$Q^{**} = 12kQ^* = 12k(\text{Pr})(Ec)\left(\frac{\partial u}{\partial y}\right)^2 ;$$

Here $r = \dfrac{k}{h^2}$ and h, k are mesh sizes along y-direction and time-direction respectively. Index 'i' refers to space and 'j' refers to the time. In the equations (13) and (14) taking i = 1(1) n and using boundary conditions (8), then the following system of equations are obtained:

$$A_i X_i = B_i \quad i = 1(1)2$$ (18)

Where $A_i^{'}$s are matrices of order n and X_i, $B_i^{'}$s are column matrices having n-components. The solutions of above system of equations are obtained by using Thomas algorithm for velocity and temperature. Also, numerical solutions for these equations are obtained by C - programme. In order to prove the convergence and stability of Galerkin finite element method, the same C - programme was run with smaller values of h and k and no significant change was observed in the values of u and T. Hence the Galerkin finite element method is stable and convergent.

Knowing the velocity field, the skin - friction at the plate in the dimensionless form is given by $\tau = \left(\dfrac{\partial u}{\partial y}\right)_{y=0}$

Knowing the temperature field, the rate of heat transfer coefficient can be obtained which in non dimensional form, in terms of the Nusselt number is given by $Nu = \left(\dfrac{\partial T}{\partial y}\right)_{y=0}$

Knowing the concentration field the rate of mass transfer coefficient can be obtained, which in the non dimensional form, in terms of Sherwood number is given by $Sh = \left(\dfrac{\partial C}{\partial y}\right)_{y=0}$

4. DISCUSSION OF THE RESULTS

The profiles of velocity, temperature and concentration are shown in the figures from (2) to (13) respectively. Figures (2) and (3) exhibit the effect of Grashof number and Modified Grashof numbers on the velocity profile with other parameters are fixed. The Grashof number (Gr) signifies the relative effect of the thermal buoyancy force to the viscous hydrodynamic force in the boundary layer. As expected, it is observed that there is a rise in the velocity due to the enhancement of thermal buoyancy force. Also, as Gr increases, the peak values of the velocity increases rapidly near the porous plate and then decays smoothly to the free stream velocity. The Modified Grashof number (Gm) defines the ratio of the species buoyancy force to the viscous hydrodynamic force. As expected, the fluid velocity increases and the peak value is more distinctive due to increase in the species buoyancy force. The velocity distribution attains a distinctive maximum value in the vicinity of the plate and then decreases properly to approach the free stream value. It is noticed that the velocity increases with increasing values of the Modified Grashof number (Gm).

Figure (4) depicts the effect of Prandtl number on velocity profiles in presence of foreign species such as Mercury ($\Pr$ = 0.025), Air ($\Pr$ = 0.71), Water ($\Pr$ = 7.00) and Methanol ($\Pr$ = 11.62) are shown in figure (4). We observe that from figure (4) the tangential velocity decreases with increasing of Prandtl number $(\Pr)$. The nature of velocity profiles in presence of foreign species such as Hydrogen (Sc = 0.22), Helium (Sc = 0.30), Oxygen (Sc = 0.60) and Water vapour (Sc = 0.66) are shown in figure (5). The flow field suffers a decrease in velocity at all points in presence of heavier diffusing species.

The effect of the Hartmann number (M) is shown in figure (6). It is observed that the velocity of the fluid decreases with the increase of the magnetic field number values. The decrease in the velocity as the Hartmann number (M) increases is because the presence of a magnetic field in an electrically conducting fluid introduces a force called the Lorentz force, which acts against the flow if the magnetic field is applied in the normal direction, as in the present study. This resistive force slows down the fluid velocity component as shown in figure (6). The influence of the viscous dissipation parameter i.e., the Eckert number (Ec) on the velocity and temperature are shown in figures (9) and (11) respectively. The Eckert number (Ec) expresses the relationship between the kinetic energy in the flow and the enthalpy. It embodies the conversion of kinetic energy into internal energy by work done against the viscous fluid stresses. Greater viscous dissipative heat causes a rise in the temperature as well as the velocity. This behavior is evident from figures (9) and (11). Figures (7) and (12) illustrate the influence of heat absorption coefficient (Q) on the velocity and temperature at t =1.0 respectively. Physically speaking, the presence of heat absorption (thermal sink) effects has the tendency to reduce the fluid temperature. This causes the thermal buoyancy effects to decrease resulting in a net reduction in the fluid velocity. These behaviors are clearly obvious from figures (7) and (12) in which both the velocity and temperature distributions decrease as (Q) increases. It is also observed that the both the hydrodynamic (velocity) and the thermal (temperature) boundary layers decrease as the heat absorption effects increase. The effect of Permeability parameter (K) is presented in the figure (8). From this figure we observe that, the velocity is increases with increasing values of K.

In figure (10) we depict the effect of Prandtl number $(\Pr)$ on the temperature field. It is observed that an increase in the Prandtl number leads to decrease in the temperature field. Also, temperature field falls more rapidly for water in comparison to air and the temperature curve is exactly linear for mercury, which is more sensible towards change in temperature. From this observation it is conclude that mercury is most effective for maintaining temperature differences and can be used efficiently in the laboratory. Air can replace mercury, the effectiveness of maintaining temperature changes are much less than mercury. However, air can be better and cheap replacement for industrial purpose. This is because, either increase of kinematic viscosity or decrease of thermal conductivity leads to increase in the value of Prandtl number $(\Pr)$. Hence temperature decreases with increasing of Prandtl number $(\Pr)$. Figure (13) shows the concentration field due to variation in Schmidt number (Sc) for the gasses Hydrogen, Helium, Water–vapour, Oxygen and Ammonia. It is observed that concentration field is steadily for Hydrogen and falls rapidly for Oxygen and Ammonia in comparison to Water–vapour. Thus Hydrogen can be used for maintaining effective concentration field and Water–vapour can be used for maintaining normal concentration field.

Table 1. Skin – friction coefficient (τ)

Gr	Gm	$\Pr$	Sc	M	Ec	Q	K	τ
1.0	1.0	0.71	0.22	1.0	0.001	1.0	1.0	3.9005
2.0	1.0	0.71	0.22	1.0	0.001	1.0	1.0	5.7162
1.0	2.0	0.71	0.22	1.0	0.001	1.0	1.0	5.9855
1.0	1.0	7.00	0.22	1.0	0.001	1.0	1.0	2.1331
1.0	1.0	0.71	0.30	1.0	0.001	1.0	1.0	3.7137
1.0	1.0	0.71	0.22	2.0	0.001	1.0	1.0	3.0999
1.0	1.0	0.71	0.22	1.0	0.100	1.0	1.0	3.9160
1.0	1.0	0.71	0.22	1.0	0.001	2.0	1.0	3.2936
1.0	1.0	0.71	0.22	1.0	0.001	1.0	2.0	4.4653

The profiles for skin – friction (τ) due to velocity under the effects of Grashof number (Gr), Modified Grashof number (Gm), Prandtl number $(\Pr)$, Schmidt number (Sc), Hartmann number (M), Eckert number (Ec), Heat absorption coefficient (Q) and Permeability parameter (K) are presented in the table 1 respectively. We observe from

this table 1, the skin – friction (τ) rises under the effects of Grashof number (Gr), Modified Grashof number (Gm), Eckert number (Ec) and Permeability parameter (K). And falls under the effects of Prandtl number (Pr), Schmidt number (Sc), Hartmann number (M) and Heat absorption coefficient (Q).

Table 2. Nusselt number (Nu) due to temperature profiles

Pr	Ec	Q	Nu
0.71	0.001	1.0	7.2153
7.00	0.001	1.0	2.0304
0.71	0.100	1.0	7.3393
0.71	0.001	2.0	6.8941

The profiles for Nusselt number (Nu) due to temperature profile under the effect of Prandtl number (Pr), Eckert number (Ec) and Heat absorption coefficient (Q) are presented in the table 2. From this table we observe that, the Nusselt number (Nu) due to temperature profile rises under the effect of Eckert number (Ec) and falls under the effects of Prandtl number (Pr) and Heat absorption coefficient (Q).

Table 3. Sherwood number (Sh) due to concentration profiles

Sc	Sh
0.22	6.8812
0.30	6.4734

The profiles for Sherwood number (Sh) due to concentration profiles under the effect of Schmidt number (Sc) is presented in the table 3. We see from this table the Sherwood number (Sh) due to concentration profile falls under the effect of Schmidt number (Sc).

5. OBSERVATIONS

We summarize below the following results of physical interest on the velocity, temperature and concentration distributions of the flow field and also on the skin – friction, rate of heat and mass transfer at the wall.]

1. A growing Hartmann number or Prandtl number or Schmidt number or Heat absorption coefficient retards the velocity of the flow field at all points.
2. The effect of increasing Grashof number or Modified Grashof number or Permeability parameter or Eckert number is to accelerate velocity of the flow field at all points.
3. A growing Prandtl number or heat absorption coefficient decreases temperature of the flow field at all points.
4. The Eckert number increases the temperature of the flow field at all points.
5. The Schmidt number decreases the concentration of the flow field at all points.
6. A growing Hartmann number or Prandtl number or Schmidt number or Heat absorption coefficient decreases the skin – friction while increasing Grashof number or Modified Grashof number or Permeability parameter or Eckert number increases the skin – friction.
7. The rate of heat transfer is decreasing with increasing of Prandtl number or heat absorption coefficient and increases with increasing of Eckert number.
8. The rate of mass transfer is decreasing with increasing of Schmidt number.

REFERENCES

[1] Ahmed, S. and Liu, I. C. Mixed convective three-dimensional heat and mass transfer flow with transversely periodic suction velocity, *International Journal of Applied Mathematics and Mechanics*, 6(1), pp. 58 – 73 (2010).
[2] Ahmed, S. Effects of viscous dissipation and chemical reaction on transient free convective MHD flow over a vertical porous plate. *Journal of Energy Heat and Mass Transfer* 32, 311-332 (2010).
[3] Ahmed, S. Free and forced convective MHD oscillatory flows over an infinite porous surface in an oscillating free stream. *Latin American Applied Research* 40, 167 - 173 (2010).
[4] Ahmed, S. Transient three – dimensional flows through a porous medium with transverse permeability oscillating with time. *Emirates Journal for Engineering Research* 13(3), 11-17 (2008).

[5]   Aldoss, T. K. and Al-Nimir, M. A. Effect of the local acceleration term on the MHD transient free convection flow over a vertical plate. *International Journal for Numerical Methods for Heat Fluid Flow* 15(3), 296-305 (2005).

[6]   Chamkha, A. J. MHD flow of a uniformly stretched vertical permeable surface in the presence of heat generation/absorption and a chemical reaction. *International Communication in Heat and Mass Transfer* 30(3), 413 - 422 (2003).

[7]   Chen, C. H. Combined heat and mass transfer in MHD free convection from a vertical plate Ohmic heating and viscous dissipation. *International Journal of Engineering and Sciences* 42(7), 699 - 713 (2004).

[8]   Crammer, K.P. and Pai, S.L., Magneto-fluid Dynamic for Engineers and Applied Physicist, *New York: Mc-Graw Hill book Co.*(1973).

[9]   Ferraro, V.C.A., Plumpton, C., An introduction to Magneto Fluid Mechanics, *Clarandon press, Oxford* (1966).

[10] Gebharat, B., and Mollendorf *J viscous dissipation in external natural convection flows, J. Fluid Mech.,* 38:pp. 97-107 (1969).

[11] Gebharat, B., Effects of viscous dissipation in natural convection *J. Fluid Mech.* 14:pp. 225-232(1962).

[12] Israel-Cookey C., Ogulu A and Omubo-Pepple V. B., Influence of viscous dissipation on unsteady MHD free convective flow past an infinite heated vertical plate in porous medium with time dependent suction, *Int. J. Heat Mss Transfer,* 46:pp.1253-1261 (1972).

[13] Muthucumaraswamy, R., Ganesan, P., and Soundalgekar, V. M. Heat and mass transfer effects on flow past an impulsively started vertical plate. *Acta Mechanica* 146 (1-2), 1-8 (2001).

[14] Prasad, V. R., N. Bhaskar Reddy and Muthucumaraswamy R., Finite difference analysis of radiative free convection flow past an impulsively started vertical plate with variable heat and mass flux. *Journal of Applied Fluid Mechanics,* 4, 1, 59 – 68 (2011).

[15] Prasad V. R., Bhaskar Reddy N., and Muthucumaraswamy R., Transient radiative hydromagnetic free convection flow past an impulsively started vertical plate with uniform heat and mass flux, *Theoretical Applied Mechanics,* 33, 1, 31 – 63(2006).

[16] Rao J. A., and Sivaiah S., chemical reaction effects on unsteady MHD flow past semi infinite vertical porous platewith viscous dissipation. *Appl. Math. Engl. Ed.,* 32(8), 1065-1078 (2011).

[17] Sahoo P. K., Datta N., Biswal s., Magnetohydrodynamic unsteady free convection flow past an infinite vertical plate with constant suction and heat sink. *Indian J. Pure Appl. Math,* 34(1) L: 145-155 (2003).

[18] Shercliff, J.A., A Text Book of Magnetohydrodynamics, London: *Pergamon Press* (1965).

[19] Singh, A. K., and Singh N. P., Heat and Mass transfer in MHD flow of a viscous fluid past a vertical plate under oscillatory suction velocity. *Ind Journal of Pure Application Math, 34*, 429 – 442(2003).

[20] Soundalgekar V. M., Viscous Dissipation effects on unsteady free convective flow past an infinite vertical porous plate with constant suction, *Int. J. Heat Mass Transfer,* 15:pp. 1253-1261 (1962).

[21] Sudheer Babu and Satyanarayana P.V., effects of chemical reaction and radiation absorption on free convective flow through porous medium with variable suction in the presence of uniform magnetic field, *JP. Journal of Heat and Mass transfer*, 3:pp. 219-234 (2009).

[22] Suneetha S., Bhaskar Reddy N., and Ramachandra Prasad V., Radiation and Mass transfer effects on MHD free convective Dissipative fluid in the presence of heat absorption/sink. *Journal of Applied Fluid Mechanics,* 4, 1, 107 – 113 (2011).
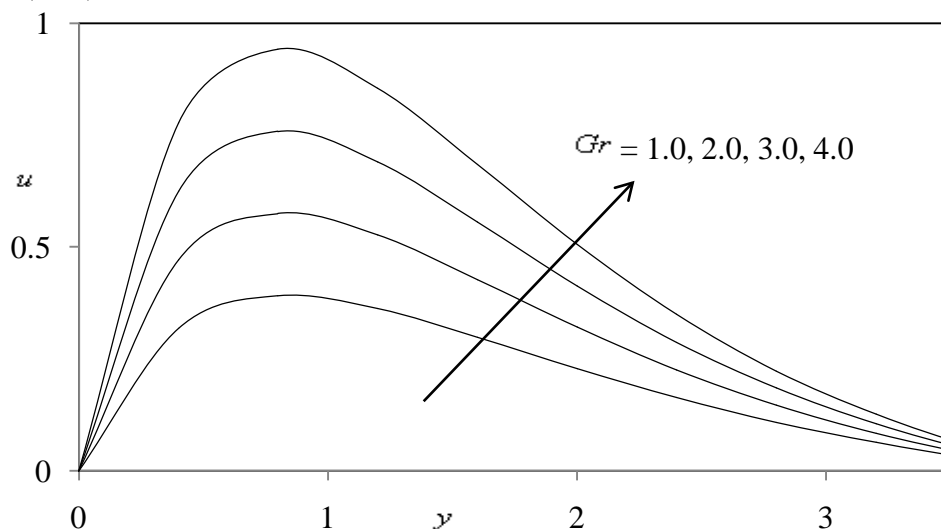

Figure 2. Effect of Gr on velocity profiles u when $Gm = 1.0$, $\text{Pr} = 0.71$, $Sc = 0.22$, $M = 1.0$, $Ec = 0.001$,

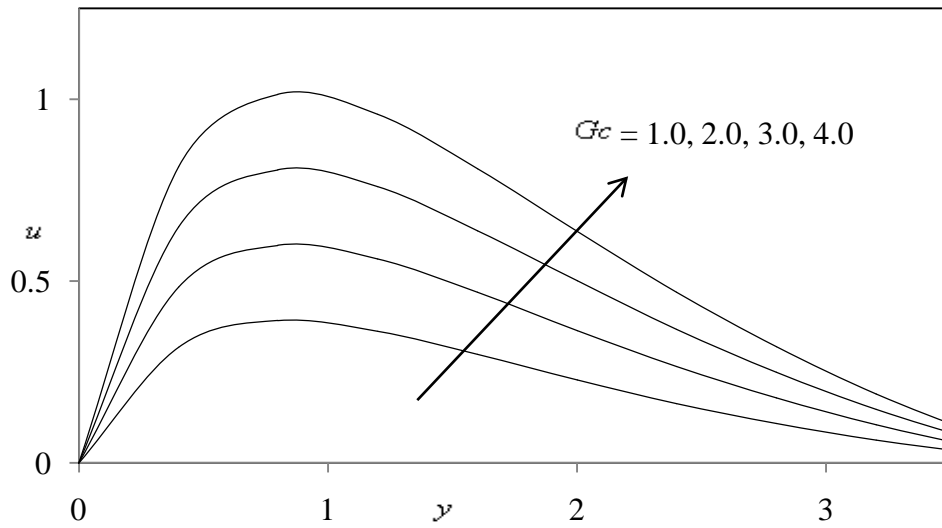$$Q = 1.0, \ K = 1.0 \text{ and } \omega t = \frac{\pi}{2}.$$

Figure 3. Effect of Gm on velocity profiles u when $Gr = 1.0$, $\text{Pr} = 0.71$, $Sc = 0.22$, $M = 1.0$, $Ec = 0.001$, $Q = 1.0$, $K = 1.0$ and $\omega t = \dfrac{\pi}{2}$.
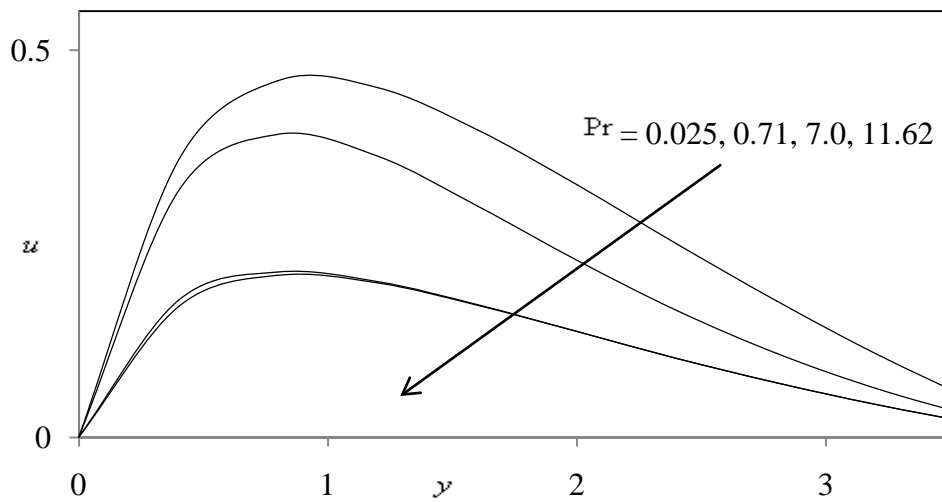

Figure 4. Effect of Pr on velocity profiles u when $Gr = 1.0$, $Gm = 1.0$, $Sc = 0.22$, $M = 1.0$, $Ec = 0.001$, $Q = 1.0$, $K = 1.0$ and $\omega t = \dfrac{\pi}{2}$.
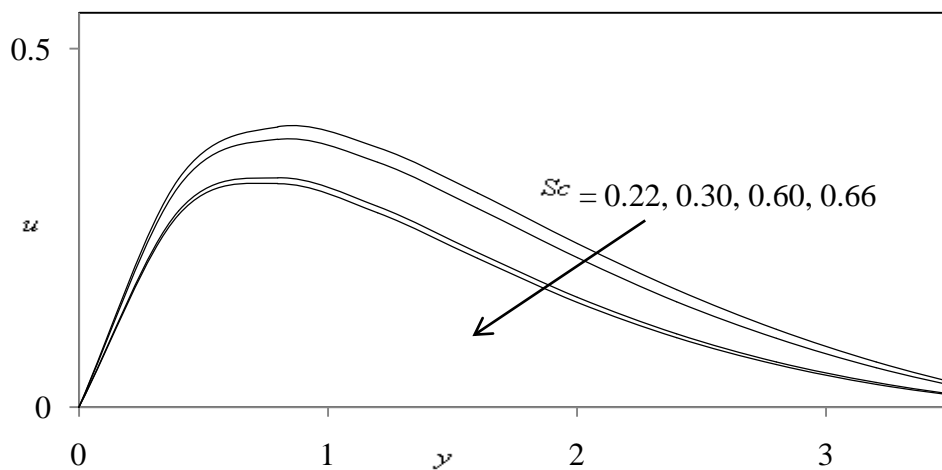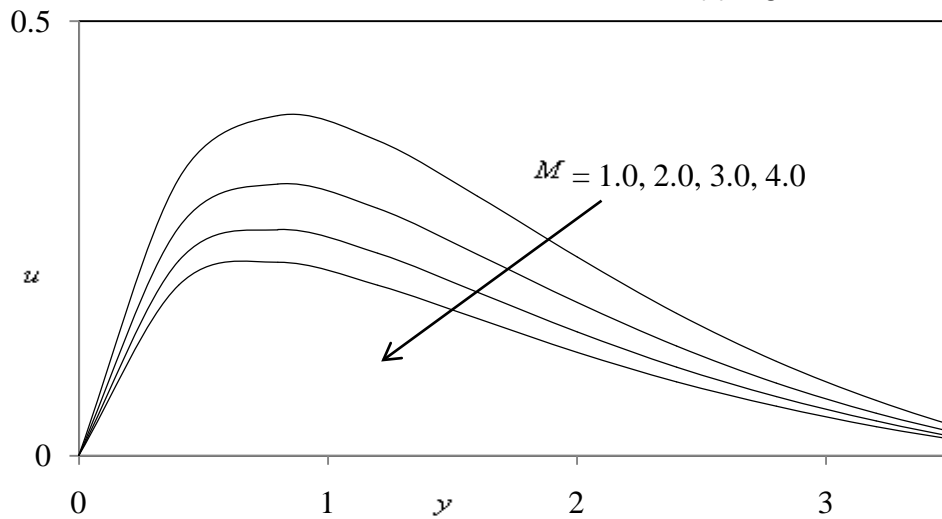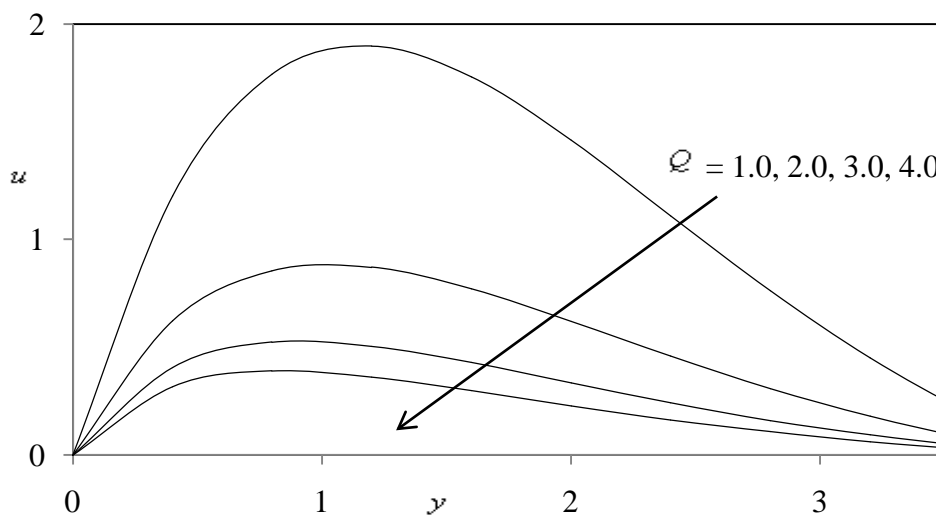

Figure 5. Effect of Sc on velocity profiles u when $Gr = 1.0$, $Gm = 1.0$, $\text{Pr} = 0.71$, $M = 1.0$, $Ec = 0.001$, $Q = 1.0$, $K = 1.0$ and $\omega t = \dfrac{\pi}{2}$.

Figure 6. Effect of M on velocity profiles u when $Gr = 1.0$, $Gm = 1.0$, $\Pr = 0.71$, $Sc = 0.22$, $Ec = 0.001$, $Q = 1.0$, $K = 1.0$ and $\omega t = \dfrac{\pi}{2}$.

Figure 7. Effect of Q on velocity profiles u when $Gr = 1.0$, $Gm = 1.0$, $\Pr = 0.71$, $Sc = 0.22$, $M = 1.0$, $Ec = 0.001$, $K = 1.0$ and $\omega t = \dfrac{\pi}{2}$.
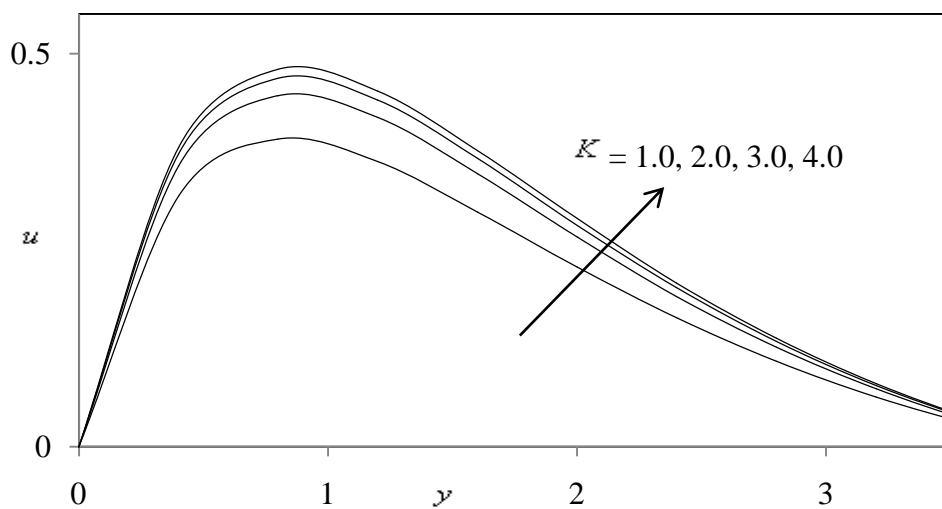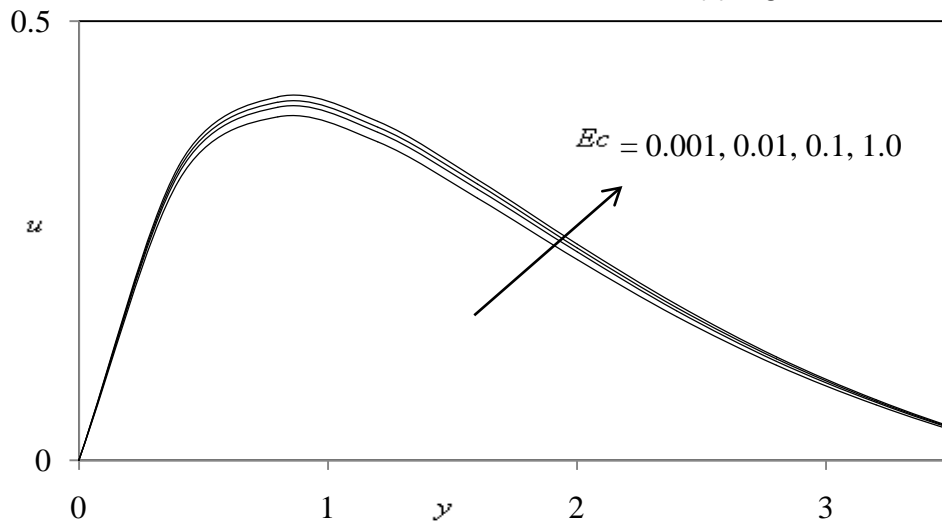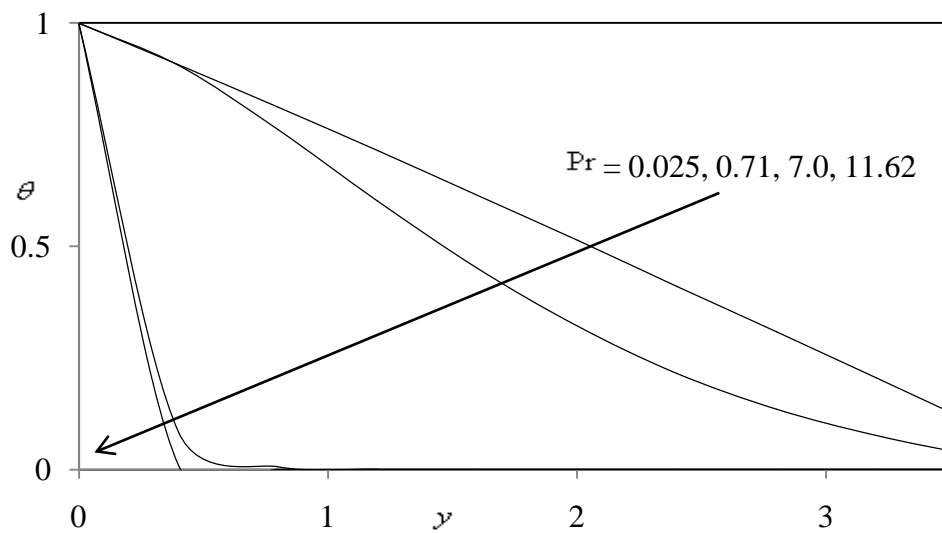

Figure 8. Effect of K on velocity profiles u when $Gr = 1.0$, $Gm = 1.0$, $\Pr = 0.71$, $Sc = 0.22$, $M = 1.0$, $Ec = 0.001$, $Q = 1.0$ and $\omega t = \dfrac{\pi}{2}$.

Figure 9. Effect of Ec on velocity profiles u when $Gr = 1.0$, $Gm = 1.0$, $\Pr = 0.71$, $Sc = 0.22$, $M = 1.0$,

$Q = 1.0$, $K = 1.0$ and $\omega t = \dfrac{\pi}{2}$.

Figure 10. Effect of $\Pr$ on temperature profiles θ when $Gr = 1.0$, $Gm = 1.0$, $Sc = 0.22$, $M = 1.0$, $Ec = 0.001$,

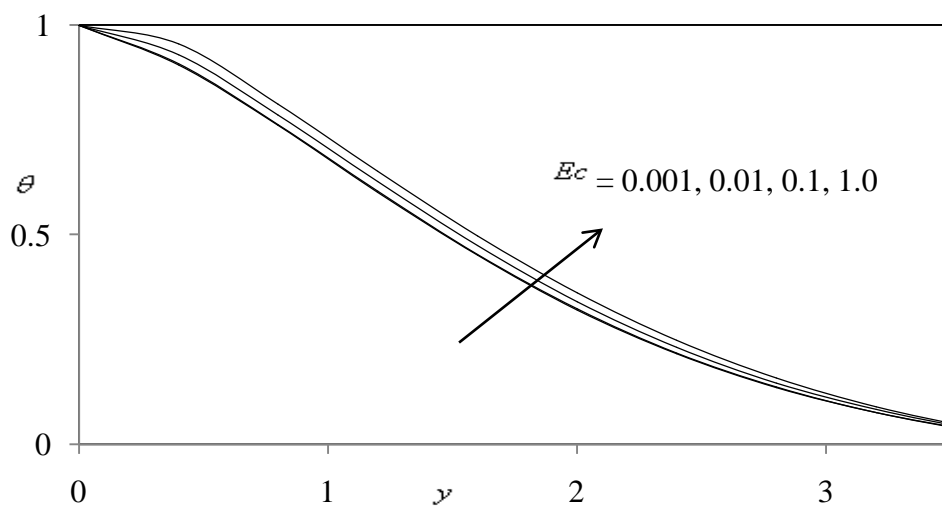$Q = 1.0$, $K = 1.0$ and $\omega t = \dfrac{\pi}{2}$.

Figure 11. Effect of Ec on temperature profiles θ when $Gr = 1.0$, $Gm = 1.0$, $\Pr = 0.71$, $Sc = 0.22$, $M = 1.0$,

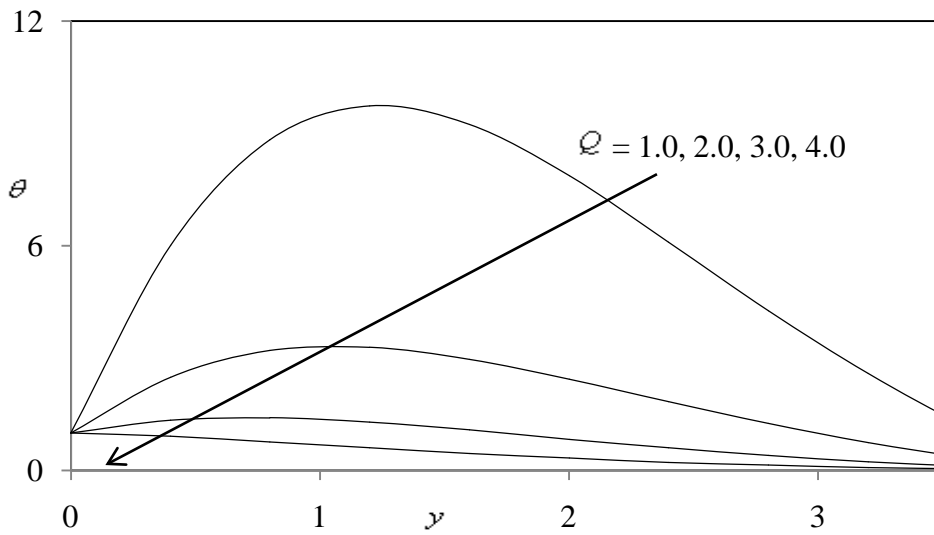$Q = 1.0$, $K = 1.0$ and $\omega t = \dfrac{\pi}{2}$.

Figure 12. Effect of Q on temperature profiles θ when $Gr = 1.0$, $Gm = 1.0$, $\text{Pr} = 0.71$, $Sc = 0.22$, $M = 1.0$,

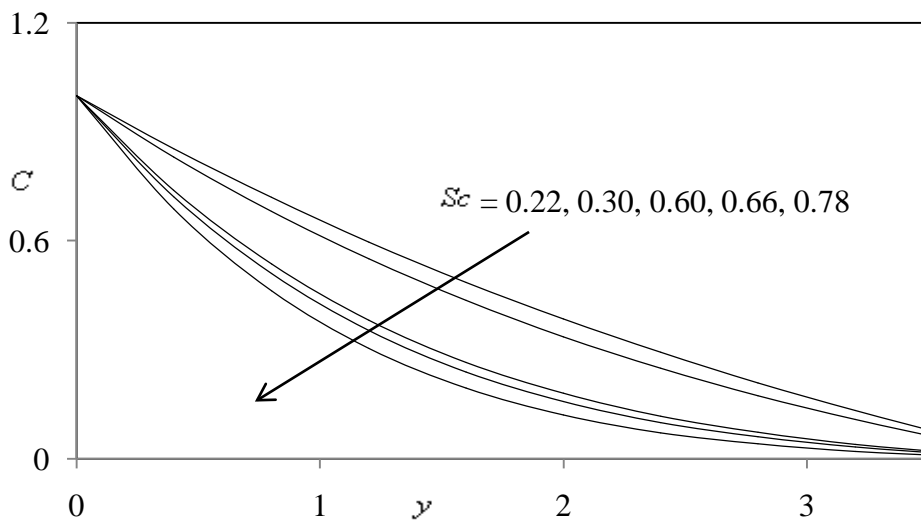$Ec = 0.001$, $K = 1.0$ and $\omega t = \dfrac{\pi}{2}$.

Figure 13. Effect of Sc on concentration profiles C when $Gr = 1.0$, $Gm = 1.0$, $\text{Pr} = 0.71$, $M = 1.0$, $Ec = 0.001$,

$Q = 1.0$, $K = 1.0$ and $\omega t = \dfrac{\pi}{2}$.

Source of support: Nil, Conflict of interest: None Declared